J Biol Inorg Chem (2015) 20:989–1004
DOI 10.1007/s00775-015-1282-2

ORIGINAL PAPER

DNA binding and cleavage studies of copper(II) complexes with 2′-deoxyadenosine modified histidine moiety

Justyna Borowska[1] · Malgorzata Sierant[2] · Elzbieta Sochacka[3] · Daniele Sanna[4] · Elzbieta Lodyga-Chruscinska[1]

Received: 12 March 2015 / Accepted: 20 June 2015 / Published online: 18 July 2015

Abstract This work is focused on the study of DNA binding and cleavage properties of 2′-deoxyadenosines modified with ester/amide of histidine (his^{6}dA ester, his^{6}dA amide) and their copper(II) complexes. To determine the coordination mode of the complex species potentiometric and spectroscopic (UV–visible, CD, EPR) studies have been performed. The analysis of electronic absorption and fluorescence spectra has been used to find the nature of the interactions between the compounds and calf thymus DNA (CT-DNA). There is significant influence of the $-NH_2$ and $-OCH_3$ groups on binding of the ligands or the complexes to DNA. Only amide derivative and its complex reveal intercalative ability. In the case of his^{6}dA ester and Cu(II)–his^{6}dA ester the main interactions can be groove binding. DNA cleavage activities of the compounds have been examined by gel electrophoresis. The copper complexes have promoted the cleavage of plasmid DNA, but none of the ligands exhibited any chemical nuclease activity. The application of different scavengers of reactive oxygen species provided a conclusion that DNA cleavage caused by copper complexes might occur via hydrolytic pathway.

Keywords Artificial nucleases · Copper complexes · Histidine derivatives

Introduction

The development of synthetic nucleases capable of accelerating the hydrolysis of DNA has attracted considerable scientific interest over the last 20 years. There are several reasons for justifying the interest in such systems. First, artificial nucleases could lead to a better understanding of the chemistry of hydrolytic enzymes, secondly, they can be used to detoxify pesticides and chemical weapons, which often have phosphate ester-like structures and, thirdly, reagents effectively hydrolyzing phosphodiester bonds can be used in molecular biology as artificial restriction enzymes. These systems are also very valuable, because they can show different sequence selectivity to cut DNA than natural nucleases [1].

Transition metal complexes due to DNA binding and cutting abilities in physiological conditions found wide applications in chemistry of nucleic acids as sequence-specific binding factors to DNA or as diagnostic agents in medical applications.

Copper belongs to the so-called bioelements and plays a critical role in biological processes. Activity of many identified enzymes requires the presence of copper in their active centers. Because of important function in cell metabolism, chemical synthesis and biological activity, copper(II)

Electronic supplementary material The online version of this article (doi:10.1007/s00775-015-1282-2) contains supplementary material, which is available to authorized users.

✉ Justyna Borowska
juustyna.pawlak@o2.pl

✉ Elzbieta Lodyga-Chruscinska
elalodyg@p.lodz.pl

[1] Institute of General Food Chemistry, Lodz University of Technology, ul. Stefanowskiego 4/10, 90-924 Lodz, Poland

[2] Centre of Molecular and Macromolecular Studies, Polish Academy of Science, ul. Sienkiewicza 112, 90-363 Lodz, Poland

[3] Institute of Organic Chemistry, Lodz University of Technology, ul. Zeromskiego 176, 90-924 Lodz, Poland

[4] Istituto C.N.R. Chimica Biomolecolare, Trav. La Crucca 3, reg. Baldinca, 07040 Sassari, Italy

complexes are the subject of research in the area of bioinorganic and biological chemistry. Studies of the fragments of nucleic acids and their complexes with copper are considered to be very important, especially in relation to biological and clinical role of these compounds [2].

Nucleosides modified with amino acid residues were used as "building blocks" of oligonucleotides with the sequence of DNA enzymes (deoxyribozymes) [3, 4]. Deoxyribozymes that contain nucleosides modified by the threonine or histamine moiety, showed an increased potential for hydrolysis of complementary RNA [5].

The selected modified nucleosides can serve as model systems to clarify the structural and functional changes occurring under the influence of transition metal ions in DNA. In our previous work, we described the physicochemical and DNA cleavage properties of his^{6}dA (histidine modified 2′-deoxyriboadenosine) and its complex with copper(II). Both the ligand and the Cu(II) complex can effectively promote cleavage of plasmid DNA in the absence of any reducing agents [6].

In the present work, we have firstly focused on finding the stoichiometry and coordinating mode of Cu(II) complexes with his^{6}dA ester or his^{6}dA amide formed in aqueous solution. Potentiometric and spectroscopic (UV–visible, CD, and EPR) studies have been performed. The second step of our research was aimed to define DNA binding efficacy and DNA cleavage activity of both ligands (his^{6}dA ester and his^{6}dA amide) and their complexes with copper(II) ions. The DNA cleavage has been found only in the case of the copper complexes. An attempt has been made to elucidate the mechanism of DNA binding and cleavage.

Materials and methods

Reagents

All chemicals were of reagent grade and were used without further purification, unless otherwise noted. Plasmid pEGFP-C1 was purchased from BD Biosciences. Agarose and ethidium bromide were obtained from Serva Electrophoresis, CT-DNA, 2′-deoxyadenosine, L-histidine were purchased from Sigma-Aldrich. Modified nucleosides: his^{6}dA amide and his^{6}dA ester were prepared according to the established procedures reported beneath. Their purity was verified by HPLC, ^{1}H NMR and high-resolution mass spectrometry to be >99 %. For the experiments, Cu(II)-L systems, where L = his^{6}dA amide, his^{6}dA ester, were prepared in aqueous solutions by mixing $CuCl_2$ and the ligands in molar ratio of 1:2, to maintain the formation of the complexes. All solutions were prepared using ultra-pure water (Mili-Q Integral Water Purification System, Merck Millipore).

Synthesis of histidine modified 2′-deoxyadenosines (his^{6}dA amide and his^{6}dA ester)

The synthesis of 2′-deoxyadenosines modified with L-histidine residue was performed according to the Scheme 1.

*Synthesis of 3′,5′-di-O-acetyl-2′-deoxyadenosine (**b**)*

To the solution of 2′-deoxyadenosine **a** (3 g, 11.95 mmol) in 40 mL of anhydrous pyridine 12 mL of acetic anhydride (119.5 mmol) were slowly dropped and the reaction mixture was stirred for 1.5 h at room temperature. Then, after cooling in the ice bath, 10 mL of CH_2Cl_2 were added and the solution was washed with 10 % aq. $NaHCO_3$ (50 mL). The aqueous layer was extracted twice with 30 mL of chloroform. The combined organic layers were dried with $MgSO_4$, the drying agent was filtered off and chloroform evaporated under reduced pressure. The resulting precipitate was three times evaporated with toluene (3 × 15 mL) and purified by crystallization from ethanol to give 3.18 g (9.5 mmol) of acetylated 2′-deoxyadenosine **b** (yield 79 %), TLC: R_f = 0.66, ($CHCl_3$/MeOH 80:20 v/v). ^{1}H NMR (250 MHz, $CDCl_3$) δ 2.09 (s, 3H, CH_3COO), 2.14 (s, 3H, CH_3COO), 2.62 (ddd, 1H, $J_{H2',H3}$ = 2.5 Hz, $J_{H2',H1'}$ = 5.9 Hz, J_{gem} = 14.1 Hz, H2′), 2.96 (ddd, 1H, $J_{H2'',H3'}$ = 6.3 Hz, $J_{H2'',H1'}$ = 8.1 Hz, J_{gem} = 14.1 Hz, H2″), 4.32–4.46 (m, 3H, H4′, H5′, H5″), 5.43 (dt, 1H, $J_{H3',H2'}$ = $J_{H3',H4'}$ = 2.5 Hz, $J_{H3',H2''}$ = 6.3 Hz, H3′) 5.85 (bs, 2H, NH-6), 6.46 (dd, 1H, $J_{H1',H2'}$ = 5.9 Hz, $J_{H1',H2''}$ = 8.1 Hz, H1), 7.99 (s, 1H, H2), 8.36 (s, 1H, H8).

*Synthesis of 3′,5′-di-O-acetyl-N^6-phenoxycarbonyl-2′-deoxyadenosine (**d**)*

3′,5′-Di-*O*-acetyl-2′-deoxyadenosine **b** (670 mg, 2 mmol) was dried by evaporation twice with 10 mL of anhydrous benzene and methylene chloride (1:1 v/v). Then dissolved in 20 mL of anhydrous methylene chloride and 1-methyl-3-phenoxycarbonylimidazolium chloride (954 mg, 4 mmol) was added. After the reaction mixture was stirred for 18 h at room temperature, the solution was evaporated in vacuum and the residue dissolved in small amount of EtOAc. Purification on a silica gel column using the same solvent as the eluent gave the nucleoside **d** in 65 % yield (579 mg, 1.3 mmol), TLC: R_f = 0.31, (EtOAc), ^{1}H NMR (250 MHz, $CDCl_3$) δ 2.07 (s, 3H, CH_3COO), 2.14 (s, 3H, CH_3COO), 2.68 (ddd, 1H, $J_{H2',H3'}$ = 2.5 Hz, $J_{H2',\ H1'}$ = 6.0 Hz, J_{gem} = 14.2 Hz, H2′), 2.98 (ddd, 1H, $J_{H2'',H3'}$ = 6.3 Hz, $J_{H2'',H1'}$ = 7.8 Hz, J_{gem} = 14.2 Hz, H2″), 4.35–4.45 (m, 3H, H4′, H5′, H5″), 5.47 (m, 1H, H3′), 6.50 (m, 1H, H1′), 6.80–7.45 (m, 5H, PhO), 8.22 (s, 1H, H2), 8.72 (bs, 1H, CONH), 8.81 (s, 1H, H8).

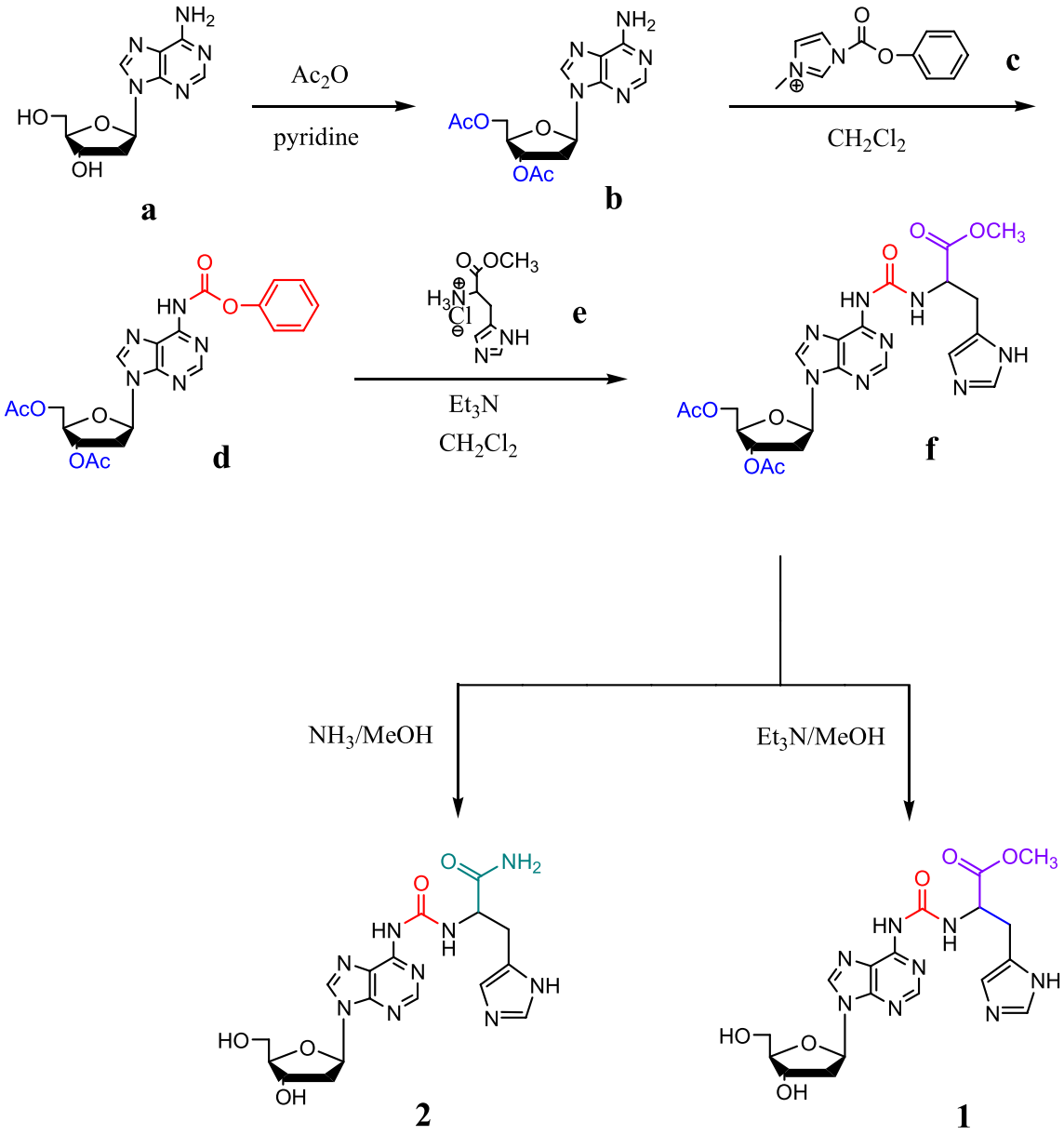

Scheme 1 Synthesis of his^{6}dA amide and his^{6}dA ester

*Synthesis of methyl ester of N2-{[9-(3′,5′-di-O-acetyl--D-2′-deoxyribofuranosyl)-9Hpurin-6-yl]-carbamoyl}-L-histidine (**f**)*

3′,5′-Di-*O*-acetyl-N^6-phenoxycarbonyl-2′-deoxyadenosine **d** (177 mg, 0.4 mmol) was dried by evaporation twice with anhydrous methylene chloride and then dissolved in the same solvent (3.6 mL). Triethylamine (124 µL, 0.88 mmol) and histidine methyl ester hydrochloride **e** (106 mg, 0.4 mmol) were added. After 1 h, TLC control ($CHCl_3$/MeOH 90:10 v/v) indicated complete reaction of substrates. The solvent was evaporated under reduced pressure. Obtained solid residue was purified by column chromatography on silica gel eluting with a gradient: 0 % MeOH in $CHCl_3$ to 10 % MeOH in $CHCl_3$. The product was obtained as white foam (173 mg, 0.32 mmol, 81 % yield). Its NMR analysis showed the presence of triethylamine. The calculated purity of the product was 81 % (final yield 66 %). Obtained compound **f**, without further purification, was used as a substrate in subsequent reactions, TLC: R_f = 0.07, ($CHCl_3$/MeOH 90:10 v/v) ^{1}H NMR (250 MHz, $CDCl_3$) δ 2.05 (s, 3H, CH_3COO), 2.15 (s, 3H, CH_3COO), 2.67 (ddd, 1H, $J_{H2',H3'}$ = 2.5 Hz, $J_{H2',H1'}$ = 5.9 Hz, J_{gem} = 14.1 Hz, H2′), 2.98 (m, 1H, H2″), 3.26–3.34 (m, 2H, CH_2-β), 3.76 (s, 3H, OCH_3), 4.13–4.42 (m, 3H, H4′, H5′, H5″), 4.94 (m, 1H, CH-α) 5.46 (m, 1H,

H3′), 6.48 (m, 1H, H1′), 6.96 (bs, 1H, Im-CH-5), 7.79 (bs, 1H, Im-CH-2), 8.44 (s, 1H, H2), 8.53 (s, 1H, H8), 9.01 (bs, 1H, CONH).

*Synthesis of methyl ester of N2-{[9-(2′-D-deoxyribofuranosyl)-9Hpurin-6-yl]-carbamoyl}-L-histidine (his^{6}dA ester) (**1**)*

Methyl ester of N2-{[9-(3′,5′-di-*O*-acetyl-D-2′-deoxyribofuranosyl)-9Hpurin-6-yl]-carbamoyl}-L-histidine **f** (140 mg, 0.26 mmol) was dissolved in 3 mL of triethylamine solution in methanol (1:9 v/v). After 3 days, TLC control indicated complete reaction of the substrate ($CHCl_3$/MeOH 80:20 v/v). The solvent was evaporated under reduced pressure and the residual solid was coevaporated with toluene. The obtained product was then purified by column chromatography on silica gel eluting with a gradient: 0 % MeOH in $CHCl_3$ to 60 % MeOH in $CHCl_3$. Traces of triethylamine left in the product were removed by coevaporation several times with methanol and toluene. The desired compound **1** was obtained as white foam (82 mg, 0.18 mmol, 68 % yield), TLC: $R_f = 0.18$, ($CHCl_3$/MeOH 80:20 v/v), HPLC: R_f = 21.95 min (XTerra® HPLC column MS C8, 5 μm 4,6 × 150 mm, flow 1 mL/min, 20 °C, detection at λ = 254 nm; gradient elution—solvent A—5 mM TEAB o pH = 7.5, solvent B = AcCN; 0–25 min from 0 to 30 % of B, 25–30 min 50 % of B); UV (H_2O): λ_{max} = 209.4 nm, ε = 25,942 dm^3 mol^{-1} cm^{-1}, λ_{max} = 269.2 nm, ε = 22 140 dm^3 mol^{-1} cm^{-1}; (HRMS, FAB): *m/z* = 447.1657, $[M + H]^+$, calculated for $C_{18}H_{23}N_8O_6$ requires 447.1662; ^{1}H NMR (250 MHz, D_2O) δ 2.43 (ddd, 1H, $J_{H3',H2'}$ = 3.4 Hz, $J_{H2',H1'}$ = 6.8 Hz, J_{gem} = 14.2 Hz, H2′), 2.69 (m, 1H, H2″), 3.17 (m, 2H, CH_2-β), 3.67 (m, 5H, CH_3, H5′, H5″), 4.04 (m. 1H, H4′), 4.52 (m, 1H, CH-α), 4.58–4.70 (signal superimposed with the signal of water molecule: H3′), 6.48 (pt, 1H, $J_{H1',H2'} = J_{H1',H2''}$ = 6.8 Hz, H1′), 7.02 (s, 1H, Im-CH-5), 7.88 (s, 1H, Im-CH-2),8.27 (s, 1H, H8), 8.28 (s, 1H, H2).

*Synthesis of amide of N2-{[9-(2′-D-deoxyribofuranosyl)-9H purin-6-yl]-carbamoyl}-L-histidine (his^{6}dA amide) (**2**)*

Methyl ester of N2-{[9-(3′,5′-di-*O*-acetyl-D-2′-deoxyribofuranosyl)-9Hpurin-6-yl]-carbamoyl}-L-histidine **f** (70 mg, 0.11 mmol) dissolved in 6 mL of methanol saturated with gaseous ammonia. After 2 days of stirring at room temperature TLC control (nBuOH/H_2O 85:15 v/v) indicated complete disappearance of the substrate. The solvent was evaporated under reduced pressure. The obtained product was purified using column chromatography on silica gel eluting with nBuOH/H_2O system (85:15 v/v). Compound **2** was obtained as white foam (17 mg, 0.04 mmol, 40 % yield), TLC: R_f = 0.4, (nBuOH/H_2O 85:15 v/v),); HPLC: R_f = 15.90 min (HPLC column and conditions the same as described for the compound **1**); UV (H_2O): λ_{max} = 209.0 nm, ε = 20 941 dm^3 mol^{-1} cm^{-1}, λ_{max} = 269.4 nm, ε = 18 274 dm^3 mol^{-1} cm^{-1}; (HRMS, FAB): *m/z* = 432.1661, $[M + H]^+$, calculated for $C_{17}H_{22}N_9O_5$ requires 432.1666; ^{1}H NMR (250 MHz, D_2O, DMSO) δ 2.40 (ddd, 1H, $J_{H2',H3'}$ = 3.6 Hz, $J_{H2',H1'}$ = 6.8 Hz, J_{gem} = 13.3 Hz, H2′), 2.71 (m, 1H, H2″), 3.05 (m, 2H, CH_2-β), 3.57 (dd, 1H, $J_{H5',H4'}$ = 4.3 Hz, J_{gem} = 12.2 Hz, H5′), 3.66 (dd, 1H, $J_{H5'',H4'}$ = 3.7 Hz, J_{gem} = 12.2 Hz, 5″), 3.96 (m, 1H, H4′), 4.25–4.51 (signals superimposed with the signal of water molecule: CH-α, H3′), 6.33 (pt, 1H, $J_{H1',H2'} = J_{H1',H2''}$ = 6.8 Hz, H1′), 6.99 (s, 1H, Im-CH-5), 7.61 (s, 1H, Im-CH-2), 8.50 (s, 1H, H2), 8.51 (s, 1H, H8).

Potentiometric measurements

The deprotonation constants of the ligands (pK_a) and the stability constants of Cu(II) complexes (log β) were determined by pH-potentiometric titrations of 2.0 mL samples. The ligand:metal molar ratio was in the range 2:1, and the concentration of Cu(II) was 1×10^{-3} M.

Measurements was carried out at 298 K and at the constant ionic strength of 0.1 M KNO_3 with a MOLSPIN pH meter (Molspin Ltd., Newcastle-upon-Tyne, UK), equipped with a digitally operated syringe (the Molspin DSI 0.250 mL) controlled by computer. The titrations were performed with a carbonate-free NaOH solution of known concentration (ca. 0.1 M) using a Russel CMAWL/S7 semi-micro combination pH electrode, calibrated for hydrogen ion concentration by the method of Irving et al. [7]. The number of experimental points was 100–150 for each titration curve. The reproducibility of the titration points included in the evaluation was within 0.005 pH units in the whole pH range examined (2–11.5). Protonation constants of the ligand and the overall stability constants of the complexes were calculated by SUPERQUAD program [8], which minimizes the sum of the weighted squared residuals between the observed and the calculated e.m.f. values. Distribution diagrams for the various systems were calculated and plotted by the program HYSS [9].

Spectroscopic measurement

UV–visible (UV–Vis) spectra were recorded with a Perkin-Elmer Lambda 11 spectrophotometer, in the same concentration range as used for the potentiometry. Circular dichroism (CD) spectra were obtained with a Jobin–Yvon CD-6 dichrograph in the ultraviolet (UV) and visible range, using 0.05 cm and 1 cm cuvettes, respectively. The spectra are expressed as $\Delta\varepsilon = \varepsilon_l - \varepsilon_r$, where ε_l and ε_r are molar absorption coefficients for left and right circularly polarized light, respectively. Anisotropic X-band EPR spectra

of frozen solutions were recorded at 120 K, using a Bruker EMX spectrometer, after the addition of ethylene glycol to ensure good glass formation. Copper(II) stock solution for EPR measurements were prepared from $CuSO_4 \cdot 5H_2O$ enriched with ^{63}Cu, to get better resolution of EPR spectra. Metallic copper (99.3 % ^{63}Cu and 0.7 % ^{65}Cu) was purchased from JV Isoflex, Moscow, Russia for this purpose and converted into the sulfate. The EPR parameters were read from the spectra (estimated uncertainties for A and g values are 1×10^{-4} cm^{-1} and 0.002, respectively, in the spectra of a single species). Measurements were performed at the maximum concentration of each species found in titrations.

DNA studies

Cleavage of double-stranded DNA

The cleavage reaction of pEGFP-C1 plasmid DNA (BD Biosciences) was carried out in the mixture containing 0.25 μg of plasmid in 5 mM Tris–HCl (pH 7.5)/5 mM NaCl buffer with various concentrations of the Cu(II) ions (0.1; 0.2; 0.5; 1; 1.5 mM), ligands (L), i.e., his^{6}dA amide and his^{6}dA ester (0.1; 0.2; 0.5; 1; 1.5 mM) or Cu(II)-L complex systems (0.1; 0.2; 0.5; 1; 1.5 mM). For the experiments, Cu(II)-L systems were prepared in aqueous solutions by mixing $CuCl_2$ and L-his^{6}dA amide or his^{6}dA ester in molar ratios of 1:2 to maintain some level of unsaturated in coordination in these labile complexes, which were then allowed to deposit for more than 5 days. Total reaction volume was 10 μL. Samples were incubated for 16 h (overnight) at 37 °C and the reaction was stopped by adding of EDTA (up to 5 mM) and the 6× loading buffer (1 % SDS, sodium dodecyl sulfate, 50 % glycerol, 0.05 % bromophenol blue, 0.05 % xylenocyanol). Finally, all samples were loaded on the 0.5 % agarose gel, containing ethidium bromide (EB), 0.5 μg/mL. Electrophoresis was carried out at 130 V in TBE (Tris–borate–EDTA) buffer. Plasmid DNA cleavage products, visible as bands in the agarose gel, were quantified and analyzed with G-BOX system (Syngene). The efficiency of the DNA cleavage was assessed by determining the ability of the species to form open circular (OC) or linear (L) plasmid forms from the supercoiled (SC) form, by quantitatively estimating the intensities of appropriate bands using the GeneTools software (Syngene).

Additionally to standard conditions of plasmid DNA cleavage, some reactions were performed in the presence of several additives: standard radical scavengers such as DMSO (0.4 M), glycerol (0.4 M), NaN_3 (10 mM) or KI (10 mM), which were included into reaction mixture before Cu(II)-L complex addition. To characterize DNA major–minor groove binding specificity of Cu(II)-L complex the reaction mixtures of typical groove binders/blockers: methyl green (0.5 mM) or DAPI (4′,6-diamidino-2-phenylindole) (8 μM) were applied. The general procedure of reaction was the same as that presented above.

Ligation of nicked pEGFP-C1

OC form of pEGFP-C1, received by the cleavage of SC form of the plasmid by Cu(II)-L system, was isolated from the reaction mixture using the agarose gel electrophoresis technique and extracted from the excised gel slice using the NucleoSpin Gel and PCR Clean-up purification system (Macherey–Nagel), according to the manufacturer's protocol. The ligation reaction was performed using 25 ng of OC form of pEGFP-C1 plasmid dissolved in water (total volume 5 μL) and equal volume of DNA Ligation Kit (Mighty Mix, Takara) containing T4 DNA ligase in the ligation buffer. The ligation mixture was incubated for 30 min at room temperature to complete reaction. Immediately, after that time the transformation of chemically competent bacteria *Escherichia coli*, strain TOP10 (Invitrogen), according to routine transformation protocol with heat shock was performed [10]. As controls for transformation procedure the (K1) untreated pEGFP-C1 plasmid; (K2) pEGFP-C1 plasmid hydrolyzed to linear form after treatment by nuclease BamHI without T4 DNA ligase or (K3) with T4 DNA ligase; and (K4) pEGFP-C1 plasmid hydrolyzed to linear form with removed phosphates at 5′ ends (alkaline phosphatase treatment, CIP—calf intestinal phosphatase) with addition of T4 DNA ligase was applied. The transformation mixtures containing competent *E. coli* bacteria suspension (200 μL) with ligation mixture (10 μL) was incubated on ice for 15 min, then tubes were put into 42 °C water bath for 30 s. and back into ice for 2 min. 500 μL of SOC medium (2 % tryptone; 0.5 % yeast extract; 10 mM NaCl; 2.5 mM KCl; 10 mM $MgCl_2$; 10 mM $MgSO_4$; 20 mM glucose) was added and each sample was incubated at 37 °C for 1 h, with gentle shaking. About 200–400 μL (7.5–15 ng of plasmid) of resulting culture was spread on the LB-agar plates (1 % tryptone; 0.5 % yeast extract; 1 % NaCl; 1.5 % agar) with kanamycin (50 μg/mL), as the selection agent, and cultured at 37 °C for 18 h, when resulted bacterial colonies were counted on each LB-agar plate.

Absorption spectra studies

Absorption spectra titrations were carried out in phosphate buffer (pH 7.5) at room temperature to investigate the binding affinity of the studied ligands or complexes toward CT-DNA. The concentration of CT-DNA was determined from the absorption intensity at 260 nm with a ε value of 6600 M^{-1} cm^{-1}. Absorption titration experiments were performed by varying the concentration of the CT-DNA

Table 1 Protonation constants (log β_{HnL}) and pK values of his^{6}dA amide and his^{6}dA ester (standard deviations are in parentheses) ($I = 0.1$ M (KNO_3), $T = 298$ K)

Ligand	log β_{HL}	log β_{h2l}	pK (N_1)	pK (N_{im})
his^{6}dA amide	6.55 (±1)	9.02 (±2)	2.47 (±2)	6.55 (±1)
his^{6}dA ester	6.52 (±1)	9.02 (±2)	2.5 (±2)	6.52 (±1)

(0–200 μM) keeping the constant concentration (10 μM) of the ligand or complex. The absorbance (A) was recorded after each addition of CT-DNA. While measuring the absorption spectra an equal amount of DNA was added to the both compound solution and the reference solution to eliminate the absorbance of the CT-DNA itself, and phosphate buffer was subtracted through baseline correction. The data were fitted to the Wolfe–Shimer equation (Eq. 1) [11] to obtain the binding constant:

$$\frac{[\text{DNA}]}{(\varepsilon_a - \varepsilon_f)} = \frac{[\text{DNA}]}{(\varepsilon_b - \varepsilon_f)} + \frac{1}{K_b(\varepsilon_b - \varepsilon_f)}, \quad (1)$$

where ε_a, ε_f, and ε_b, are the apparent, free and bound metal complex extinction coefficients, respectively. In particular ε_f was determined by a calibration curve of the isolated metal complex in aqueous solution, ε_a was determined as the ratio between the measured absorbance and the samples concentration, $A/[M]$. A plot of $[\text{DNA}]/(\varepsilon_b - \varepsilon_f)$ versus DNA gave a slope of $+1/(\varepsilon_b - \varepsilon_f)$ and a Y intercept equal to $1/K_b(\varepsilon_b - \varepsilon_f)$ [12].

Fluorescence studies

The competitive binding experiments were carried out in Tris–HCl buffer (pH 7.2) by keeping EB-DNA solution containing [EB] = 10 μM and [DNA] = 25 μM as constant and varying the concentration of ligand or complex (0–200 μM). Stern–Volmer quenching constant K_{SV} of the ligands and complexes to CT-DNA [12] were determined from the equation

$$I_0/I = 1 + K_{SV}[Q], \quad (2)$$

where I_0 and I are the fluorescence intensities of EB-DNA in the absence and the presence of the studied compounds, respectively. K_{SV} is a linear Stern–Volmer quenching constant and $[Q]$ is concentration of quencher. In the linear fit the plot of I_0/I vs $[Q]$, K_{SV} is given by the ratio of slope to intercept.

The apparent binding constants were calculated using

$$K_{app} = K_{EB} \times C_{EB}/C_{50}, \quad (3)$$

where C_{50} is the concentration of the complex that causes 50 % reduction of the initial fluorescence of EB-DNA emission intensity, K_{EB} is the binding constant of EB ($K_{EB} = 1.0 \times 10^7$ M^{-1}) and C_{EB} is the concentration of EB (10 μM) [13].

Table 2 Stability constants (logβ) of complexes in Cu(II)–his^{6}dA amide and Cu(II)–his^{6}dA ester systems (standard deviations are in parentheses) ($I = 0.1$ M (KNO_3), $T = 298$ K)

Species	pH	Log β	
		His^{6}dA amide	His^{6}dA ester
CuL_2	4.5	10.60 (±2)	10.54 (±2)
$CuLH_{-1}$	5.5	0.29 (±3)	0.69 (±3)
CuL_2H_{-1}	7.0	4.47 (±2)	5.81 (±2)
CuL_2H_{-2}	9.5	−3.99 (±3)	−2.87 (±3)

The binding stoichiometry (n), for the ligands and the complexes with Cu(II), were calculated using

$$\log[(I^0 - I)/I] = \log K_b + n \log[Q], \quad (4)$$

where K_b is the binding constant of ligands and their complexes with DNA and n is the number of binding sites. From the plot of $\log[(I^0 - I/I)]$ versus $\log[Q]$ the number of binding sites n have been obtained [12].

Results and discussion

Characterization of the ligands and their copper(II) complexes

The protonation constants of the two ligands (his^{6}dA amide and his^{6}dA ester), the stoichiometry and overall stability constants of their Cu(II) complexes were determined by potentiometric titration (Table 1, 2).

The ligands may dissociate two protons (Scheme 2). In strong acidic region the first one can be derived from purine nitrogen N(1) while in neutral pH the second one from the imidazole ring N_{im} of histidine. The acidity of N(1) nitrogen is lower and that of N_{im} donor atom is higher as compared to the values found for his^{6}dA, 1.97 and 7.05, respectively [14].

The acidity of N(1) nitrogen donor atom depends both on the presence of ureido group and on the nature of substituents as well [15]. It seems that the both groups –OCH_3 and –NH_2 influence electron density distribution in the ligand molecules leading to the changes of ionization constants.

In Cu(II)–his^{6}dA amide and Cu(II–his^{6}dA ester systems protonated species have not been found probably because that they are forming in a very small extent undetectable by potentiometry. The detectable complex formation reactions start in acidic solution (pH > 3). The ligand behaves as tridentate with three protons released from purine N(1), imidazole N_{im} and ureido N_{am} groups, respectively.

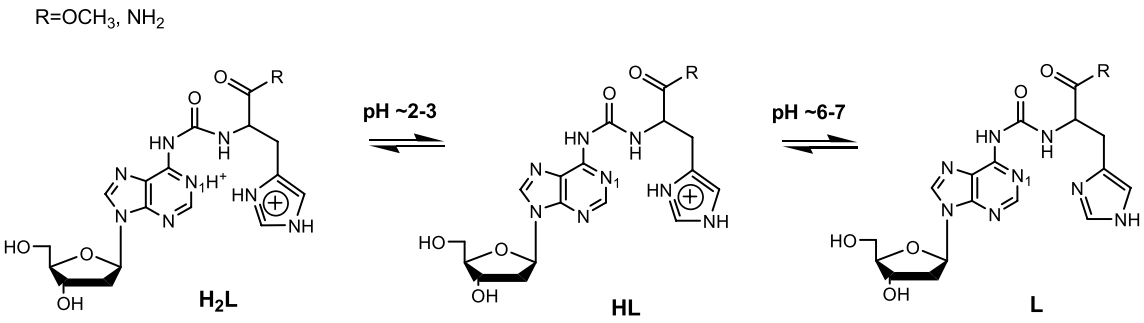

Scheme 2 Protonation and deprotonation equilibria for the ligands. The charges of the ligand species have been omitted for simplicity

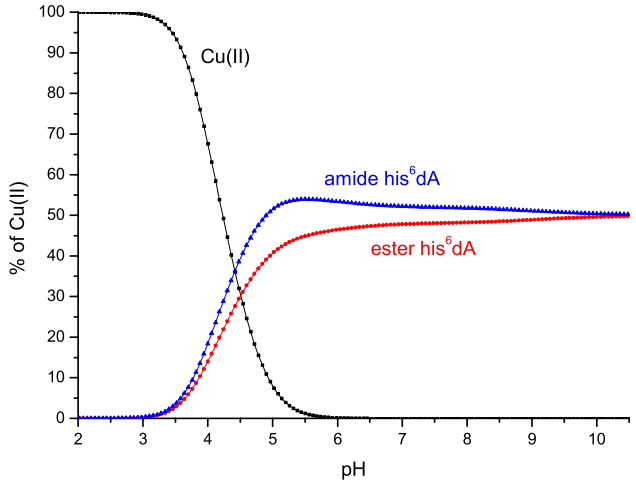

Fig. 1 Comparison of copper(II) binding efficiency by his^{6}dA amide and his^{6}dA ester. Metal to ligands molar ratio, Cu(II):his^{6}dA amide:his^{6}dA ester/1:1:1. The concentrations of the metal and the ligands were 1×10^{-3} M

Mono- and bis-complexes are indicated by potentiometric data. The presence of $-OCH_3$ or $-NH_2$ group in histidine moiety results in similar coordinating ability of deoxyadenosine ligands. The comparison of binding efficiency of the ligands indicates that his^{6}dA amide is more competitive and efficient in comparison to his^{6}dA ester over a pH range of 4–9 (Fig. 1). Also the sequestration of copper(II) ions between amide and ester of his^{6}dA (52 and 47 %, respectively) confirms the better chelating efficacy of the amide especially around neutral pH.

In the whole studied pH region the stoichiometry of the dominating copper complexes with modified deoxyadenosines was Cu(II):Ligand 1:2 (Fig. S1). The only difference between them is the protonation state of the ligand. In acidic pH a CuL_2 complex was indentified with coordination sphere of metal ion composed of {2N(1), $2N_{im}$} two nitrogen atoms derived from purine base and histidine ring. The visible spectra with the λ_{max} band localized at 657 nm in UV–Vis and 665 nm in CD Vis region and EPR parameters (Table 3) support this coordination mode which is identical to that found in his^{6}dA or histam^{6}dA nucleosides [14, 16].

At neutral pH also four nitrogen donor atoms can be identified but one of them N^-_{am} is derived from the amide of ureido group. In alkaline solution the 4N donor atoms still exist with two N^-_{am} involved in Cu(II) coordination (Fig. 2).

The charge transfer transitions visible in UV CD spectra at 326 and 320 nm, respectively, and EPR parameters (Table 3) clearly support the proposed coordination atom sets (Figs. S2 and S3).

DNA studies

Cleavage of double-stranded DNA

Supercoiled plasmid DNA cleavage by the ligands and their Cu(II) complexes was studied in the absence of oxidant like H_2O_2 or any reducing agents. Cu(II)–his^{6}dA amide and Cu(II)–his^{6}dA ester complexes are capable to cleave double-stranded DNA (dsDNA) at physiological pH and temperature as it was found in Cu(II)–his^{6}dA system [14]. When pEGFP-C1 plasmid DNA was incubated with Cu(II)–his^{6}dA amide or with Cu(II)–his^{6}dA ester, the form I (SC) of the plasmid was hydrolyzed to the form II (OC). A single cut/nick of DNA strand relaxes the supercoiling structure of the plasmid and leads to the form II. Figure 3 presents the agarose gel electrophoresis patterns for the cleavage of pEGFP-C1 plasmid after 16 h treatment with Cu(II)–his^{6}dA amide (a) or Cu(II)–his^{6}dA ester (b) solutions. The concentration of Cu(II)–his^{6}dA amide and Cu(II)–his^{6}dA ester complexes in the reaction mixture varied from 0 to 1.5 mM. The increasingly stronger conversions of form I to form II of plasmid were observed with the increase of concentration of Cu(II)–his^{6}dA amide or Cu(II)–his^{6}dA ester complexes, with the total disappearance of the both plasmid forms at the highest concentrations of Cu(II)–his^{6}dA amide (1.0 and 1.5 mM) or Cu(II)–his^{6}dA ester (1.5 mM). It is very likely due to a strong binding of the complexes to the plasmid DNA (Fig. 3a, b, lines 5 and 6) and therefore the much slower migration of the plasmid forms can be observed in the agarose gel.

Table 3 Spectroscopic parameters of copper complexes with his^{6}dA ester and his^{6}dA amide

Species	pH	Coordination mode	Spectroscopic parameters					
			EPR		UV–Vis		CD	
			$G_{\|\|}$	$A_{\|\|}$ (10^{-4} cm^{-1})	λ (nm)	ε (dm^3 cm^{-1} M^{-1})	λ (nm)	Δε (dm^3 cm^{-1} M^{-1})
CuL_2	4–5	{2N(1), $2N_{im}$}	2.262[a]	182.1[a]	656[a]	87[a]	219[a]	1.978[a]
			2.268[b]	180.0[b]	657[b]	58[b]	277	5.631
							330	0.146
							665	−0.088
							209[b]	1.620[b]
							280	0.596
							332	0.035
							668	−0.011
CuL_2H_{-1}	7.00	{N(1), N^-_{am}, $2N_{im}$}	2.241[a]	194.3[a]	613[a]	96[a]	220[a]	3.476[a]
			2.248[b]	192.7[b]	629[b]	78[b]	252	3.263
							276	6.469
							327	0.320
							582	−0.098
							733	0.025
							215[b]	2.706[b]
							277	1.307
							326	0.058
							653	−0.058
CuL_2H_{-2}	9.50	{$2N^-_{am}$, $2N_{im}$}	2.241[a]	194.3[a]	595[a]	120[a]	247[a]	3.248[a]
			2.248[b]	192.7[b]	598[b]	102[b]	289	−0.667
							323	0.529
							571	−0.145
							733	0.025
							215[b]	1.042[b]
							276	0.954
							320	0.244
							385	0.085
							591	−0.026

[a] Cu–his^{6}dA amide

[b] his^{6}dA ester

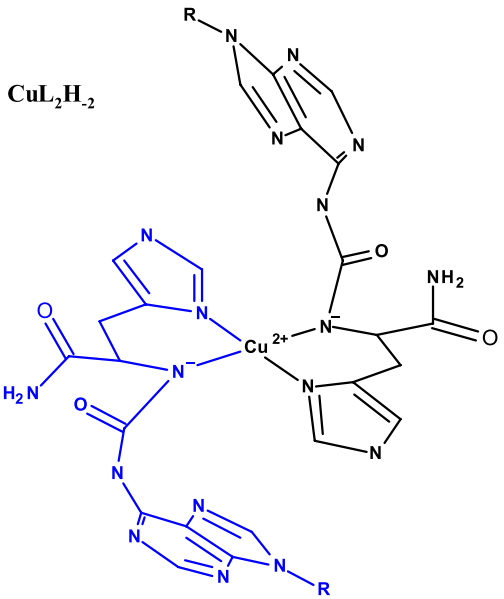

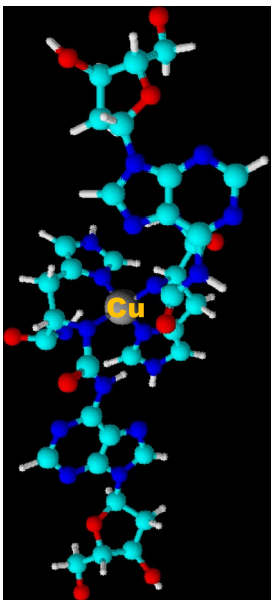

Fig. 2 Proposed structure of CuL_2H_{-2} complex. The *white inset* shows 4N donor atom set {N(1), N^-_{am}, $2N_{im}$}; R = 2′-deoxyribose; L- his^{6}dA amide

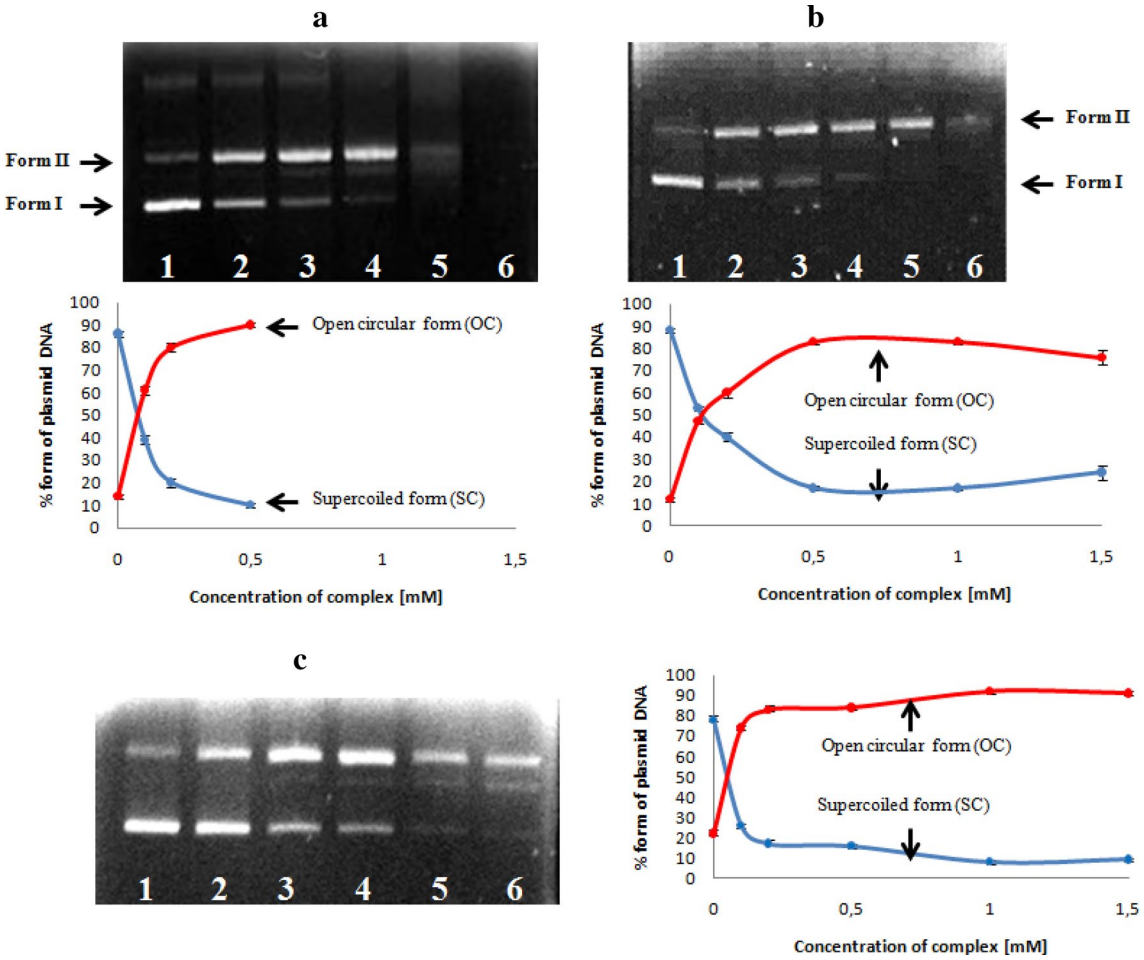

Fig. 3 Agarose gel electrophoresis patterns for the cleavage of pEGFP-C1 plasmid DNA by Cu(II)–his^{6}dA amide complex (**a**), Cu(II)–his^{6}dA ester complex (**b**) or Cu(II)–his^{6}dA complex (**c**) used in various concentrations (0, 0.1, 0.2, 0.5, 1 and 1.5 mM); *Line 1* control untreated plasmid DNA; *line 2* plasmid DNA + 0.1 mM (**a**), (**b**) or (**c**); *line 3* plasmid DNA + 0.2 mM (**a**), (**b**) or (**c**); *line 4* plasmid DNA + 0.5 mM (**a**), (**b**) or (**c**); *line 5* plasmid DNA + 1.0 mM (**a**), (**b**) or (**c**); *line 6* plasmid DNA + 1.5 mM (**a**), (**b**) or (**c**). The inserted *graphs* present the changes of the supercoiled (SC) and open circular (OC) form of DNA. Presented data are the average from three independent repeats of the plasmid DNA cleavage reaction

The extent of DNA cleavage was quantified using the GeneTools software. The results are summarized in Table S1 (Supplementary material). With respect to them one can conclude that up to the concentration of 0.2 mM the cleavage efficiency of Cu(II)–his^{6}dA amide and Cu–his^{6}dA complexes is similar unlike that of Cu(II)–his^{6}dA ester which is noticeably weaker. Above this concentration the cleavage and binding efficacy of Cu(II)–his^{6}dA amide to DNA is the strongest one. Free ligands his^{6}dA amide and his^{6}dA ester were unable to cut plasmid DNA (Fig. S4). Free Cu(II) ions have produced hardly any cleavage of plasmid DNA under the concentrations studied [17–19]. The results suggest that the Cu(II)–his^{6}dA amide, Cu(II)–his^{6}dA ester and Cu(II)–his^{6}dA complexes are the species responsible for the cleavage of plasmid DNA.

The mechanism of pEGFP-C1 DNA cleavage induced by the complexes was studied using various inhibiting agents. The reaction course was investigated in the presence of hydroxyl radical scavengers (DMSO, glycerol), singlet oxygen quencher (NaN_3) and hydrogen peroxide scavenger (KI) under experimental conditions. Figure 4 shows no inhibition in the DNA cleavage activity of the Cu(II)–his^{6}dA amide, Cu(II)–his^{6}dA ester or Cu(II)–his^{6}dA complexes in the presence of hydroxyl radical or hydrogen peroxide scavengers (lines 3–5).

Slight inhibition in DNA cleavage was observed in the presence of singlet oxygen quencher.

It suggests that the singlet oxygen species might be involved in an oxidative cleavage pathway. However, the involvement of singlet oxygen is rather doubtful in the

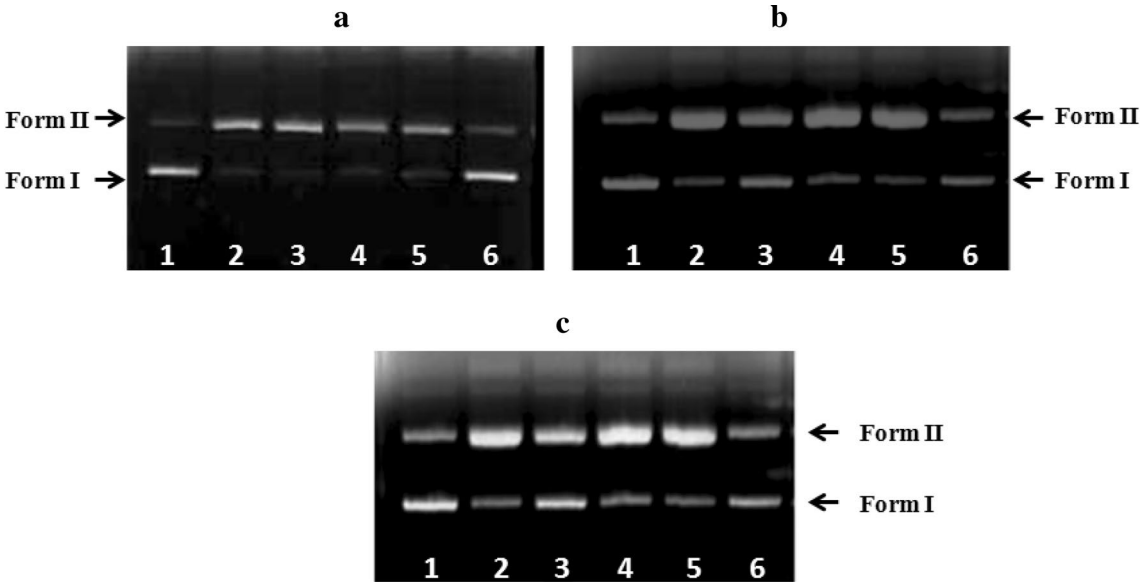

Fig. 4 Cleavage of pEGFP-C1 plasmid DNA by Cu(II)–his^{6}dA amide complex (**a**), Cu(II)–his^{6}dA ester complex (**b**) or Cu(II)–his^{6}dA (**c**) (0.2 mM) in the presence of radical scavengers in 5 mM Tris–HCl (pH 7.5)/5 mM NaCl buffer. *Line 1* control untreated plasmid DNA; *line 2* plasmid DNA + studied complexes; *line 3* plasmid DNA + DMSO (0.4 M) + studied complexes; *line 4* DNA + glycerol (0.4 M) + studied complexes; *line 5* DNA + KI (10 mM) + studied complexes; *line 6* DNA + NaN_3 (10 mM) + studied complexes

studied systems because this reactive form of oxygen is usually photogenerated and in our DNA-cleavage studies we have not used such a process. Furthermore, according to some earlier publications, this result should not be interpreted as an indication that $^1O_2$ is also participating in the process; it is probably due to the affinity of sodium azide for transition metals [20]. It was also evidenced in many publications that Cu(II) complexes [e.g., Cu(L-His)] [17] readily cleave plasmid DNA via the hydrolytic pathway [21]. Taking all this into account one can suppose a hydrolytic mechanism of DNA cleavage by the complexes studied.

The potential binding sites of the Cu(II)–his^{6}dA amide, Cu(II)–his^{6}dA ester and Cu(II)–his^{6}dA complexes with supercoiled plasmid pEGFP-C1 DNA were investigated using minor and major groove binders DAPI and MG, respectively. The supercoiled DNA was treated separately with DAPI or MG prior to the addition of the complexes. The agarose gel electrophoresis pattern shown in Fig. 5b clearly demonstrates that DAPI inhibits the DNA cleavage activity of Cu(II)–his^{6}dA ester, suggesting that the minor groove of double helix of DNA is the preferred site of the interaction with this complex. In contrast, the DNA cleavage activity of Cu(II)–his^{6}dA amide and Cu(II)–his^{6}dA complexes is inhibited after the addition of MG, suggesting that these complexes have an affinity to DNA major groove. It is very likely that the steric clashes with DNA exterior caused by the ligands or their complexes with Cu(II) ions dictate their DNA-binding mode to be surface binding to minor or major groove.

Ligation of nicked pEGFP-C1

For further studies on the mechanism of DNA cleavage the Cu(II)–his^{6}dA amide complex was selected due to its stronger interactions with DNA as compared to other complexes. In order to confirm the hydrolytic mechanism of plasmid DNA cleavage by the studied compounds, nicked (OC) form II of plasmid DNA, obtained by the action of the Cu(II)–his^{6}dA amide complex, was ligated using T4 DNA ligase and transformed into *E. coli* competent cells. The examples of successful ligation experiments, especially conversion of linear form of plasmid, result of action of artificial chemical nucleases, into relaxed open circular form of plasmid can be already found at the literature [22]. But in the case of dsDNA reaction with the studied compounds, only nicked, relaxed form II, open circular OC plasmid was observed. The linear form of plasmid has been never achieved. Because both forms of plasmid: nicked and relaxed, migrate in the agarose gel as one OC form II, it was impossible to observe any results of ligation of nicked strands of plasmid. Therefore, the *E. coli* transformation method and analysis of the number of obtained bacterial colonies were chosen for identification of hydrolytic or oxidative mechanism of Cu(II)–his^{6}dA amide complex action. Bacterial transformation allows to distinguish the both plasmid moieties: the relaxed form with repaired by T4 DNA ligase single strand breaks—which can be amplified in the bacterial cells, and the plasmid with 5′ or 3′ ends damaged during cleavage reaction, which are impossible to

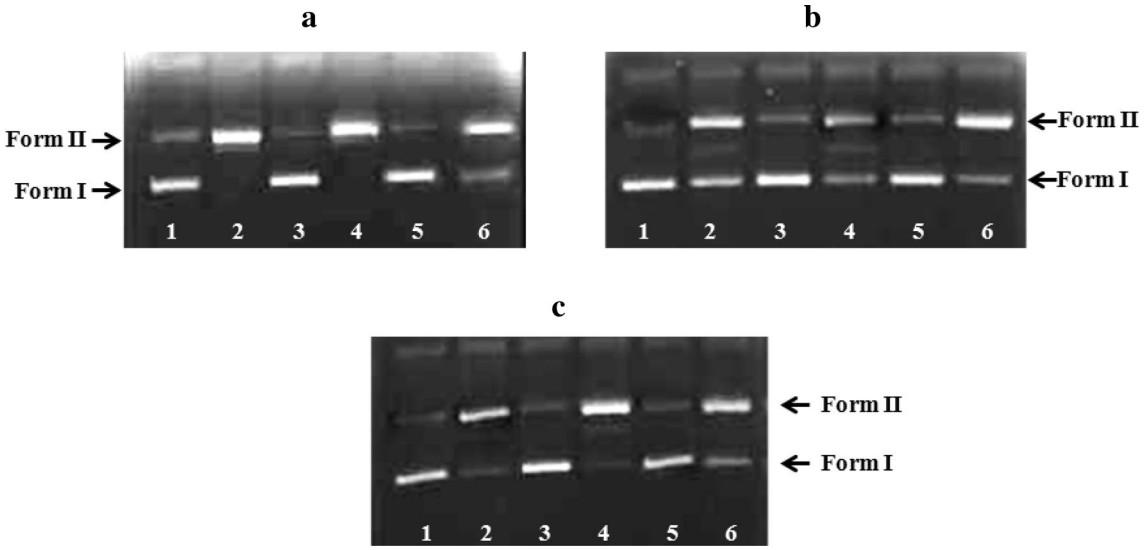

Fig. 5 Cleavage of pEGFP-C1 plasmid DNA by Cu(II)–his^{6}dA amide complex (**a**), Cu(II)–his^{6}dA ester complex (**b**) or Cu(II)–his^{6}dA (**c**) (0.2 mM) in the presence of DNA groove recognition agents, reaction performed in 5 mM Tris–HCl (pH 7.5)/5 mM NaCl buffer. *Line 1* control untreated plasmid DNA; *line 2* plasmid DNA + studied complexes; *line 3* plasmid DNA + DAPI (8 μM); *line 4* plasmid DNA + DAPI (8 μM) + studied complexes; *line 5* plasmid DNA + MG (0.5 mM); *line 6* plasmid DNA + MG (0.5 mM) + studied complexes

repair by T4 DNA ligase or another intracellular enzymatic activity. Because pEGFP-C1 plasmid has the kanamycin resistance gene, transformation mixtures were applied onto LB-agar plates containing the kanamycin as the selection factor for bacteria cells containing plasmid. After transformation, *E. coli* cells acquired a resistance to kanamycin and they were able to grow on the medium containing this antibiotic. After 20 h of incubation the bacterial colony growth was observed on the plates. Four additional samples as controls of ligation and transformation procedures were applied (Fig. 6): (K1) untreated supercoiled pEGFP-C1 plasmid DNA, (K2) pEGFP-C1 plasmid hydrolyzed to linear form by restriction nuclease (BamHI) without addition of T4 DNA ligase or (K3) with T4 DNA ligase, and (K4) pEGFP-C1 plasmid hydrolyzed to linear form by restriction nuclease (Bam HI), after dephosphorylation of 5′ end catalyzed by alkaline phosphatase, and after T4 DNA ligase treatment—the negative control of ligation. Positive transformation results for K3 sample support the correct action of T4 DNA ligase, which is able to join the ends of linear form of plasmid after hydrolytic cleavage by the restriction nuclease. Negative transformation results for K4 sample indicate that T4 DNA ligase is not able to combine the damaged (without 5′-phosphates) ends of plasmid. No bacterial colonies were observed on the LB-agar plates after transformation of samples containing the plasmid (OC form) cleaved by the complex (Cu(II)–his^{6}dA amide) with or without T4 DNA ligase (K5 and K6). It suggests that neither the T4 DNA ligase nor bacteria itself are able to ligate the forms of pEGFP-C1 nicked during the reaction with the complex, uptake them and amplify inside the cell. However, after 2 weeks the bacterial colony growth was observed on the plates K5 and K6 (K7, K8) (Fig. 6). One of the reasons why the hydrolytic properties have not been disclosed at the same time as that observed for K3 sample might be due to non structure-selective DNA cleavage induced by the complex as that of the BamHI nuclease therefore the T4 ligase could not ligate DNA in a proper manner. It may indicate lack of cohesive termini and that is why it makes end ligation more complex and significantly slower.

From all the results related to DNA cleavage is difficult to unequivocally indicate that the cleavage occurs via the hydrolytic pathway. Oxidative mechanism may not be excluded as well although we have not determined the involvement of hydroxyl radical or hydrogen peroxide in DNA cleavage. The involvement of singlet oxygen is rather impossible because this reactive form of oxygen is usually photogenerated and in our DNA-cleavage studies we have not used such a process.

Absorption spectral studies

Transition metal complexes can bind to DNA via both covalent and/or non-covalent (intercalation, electrostatic and groove binding) interactions [23]. The binding of an intercalative molecule to DNA can be characterized by notable intensity decrease (hypochromism) and red shift (bathochromism) of the electronic spectral bands. On the other hand, metal complexes, which do not intercalate or

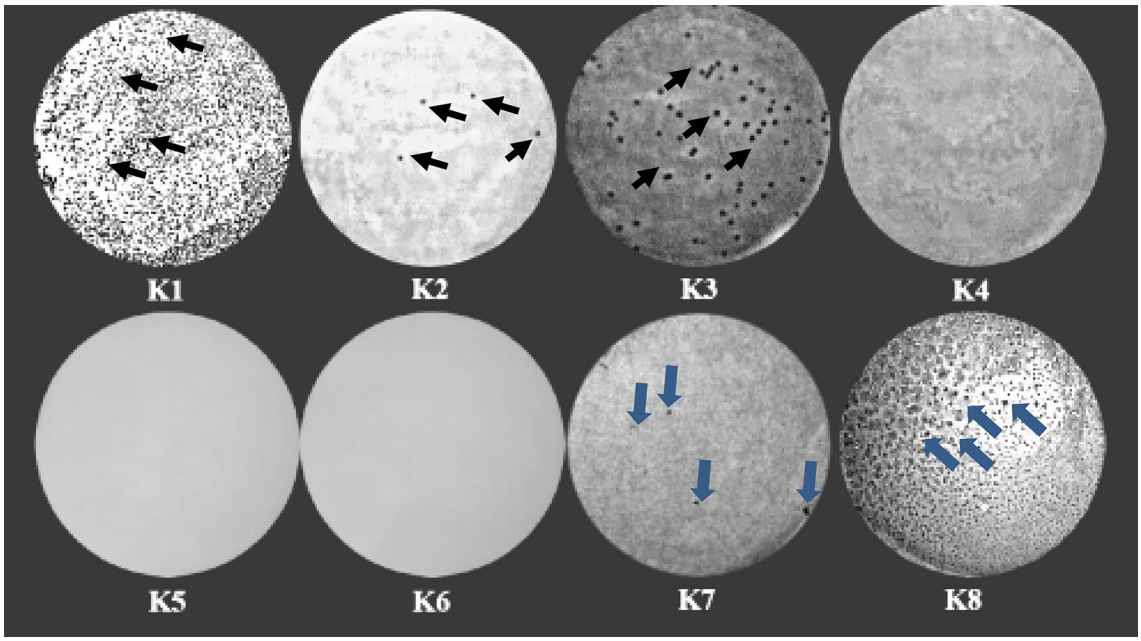

Fig. 6 LB-agar plates of studied systems: *K1* untreated pEGFP-C1; *K2* pEGFP-C1 + BamHI; *K3* pEGFP-C1 + BamHI + T4 ligase; *K4* pEGFP-C1 + BamHI + alkaline phosphatase; *K5* Cu(II)–his^{6}dA amide; *K6* Cu(II)–his^{6}dA amide + T4 ligase; *K7* and *K8* are *K5* and *K6* after keeping at the temperature of 4 °C for several weeks

interact electrostatically with DNA may exhibit hyperchromism [24]. The interactions of the ligands and their Cu(II) complexes with CT-DNA were monitored by UV–visible spectroscopy. The absorption spectra of the studied compounds in aqueous solutions were compared in the absence and in the presence of CT-DNA. Electronic absorption spectral data upon addition of CT-DNA and the binding constants are given in Fig. 7 and Table 4, respectively.

In the presence of increasing amounts of CT-DNA, UV–Vis absorption spectra of all studied compounds show slight blue shift and hyperchromism (Fig. 7). This hyperchromism can be attributed to external contact (surface binding) with the duplex which could involve hydrogen bonds of the oxygen or nitrogen atoms on the ligand with DNA nucleobases, or electrostatic interactions between the cationic species of the complexes and the negatively charged phosphate groups on the DNA backbone. The results suggest that the ligands and the complexes can bind to CT-DNA via a groove-binding mode [25, 26]. It is also consistent with the gel electrophoresis data (Fig. 5). In order to quantitatively compare the binding affinity of the compounds with CT-DNA, the intrinsic binding constants (K_b) were determined according to the Eq. 1 by monitoring the absorbance changes of the ligands and their complexes with increasing concentration of CT-DNA. The K_b values indicate the following order of binding affinity of the compounds his^{6}dA amide > Cu(II)–his^{6}dA amide > Cu(II)–his^{6}dA ester > his^{6}dA ester. The determined K_b values are much lower than those observed for typical classical intercalators (ethidium bromide, EB, $K_b = 1.4 \times 10^6$ M^{-1} in 25 mM Tris–HCl/40 mM NaCl buffer, pH 7.2) [22]. Only in the case of his^{6}dA amide and Cu(II)–his^{6}dA amide one can suppose that the ligand or the complex can be involved in partial intercalative interactions as it was found for many other compounds with the same order of K_b values [27–29].

Fluorescence spectral studies

In order to get more insight into the interaction mode of the ligand or the complexes towards DNA, the fluorescence titration experiments have been performed. The fluorescence titrations, especially the EB fluorescence displacement experiments, have been widely used to characterize the interaction of compounds with DNA by following the changes in fluorescence intensity [30]. The method is based on a decrease of fluorescence resulting from the displacement of EB from a DNA sequence by a quencher and the quenching is due to the reduction of the number of binding sites in the DNA available to the EB [31]. The intrinsic fluorescence intensity of DNA and that of EB are low, while the fluorescence intensity of EB will be enhanced on addition of DNA due to its intercalation into the DNA. Therefore, EB can be used to probe the interaction of the ligands or complexes with DNA. In our experiments, as depicted in Fig. 8 for his^{6}dA ester (**a**), Cu(II)–his^{6}dA ester (**b**), his^{6}dA amide

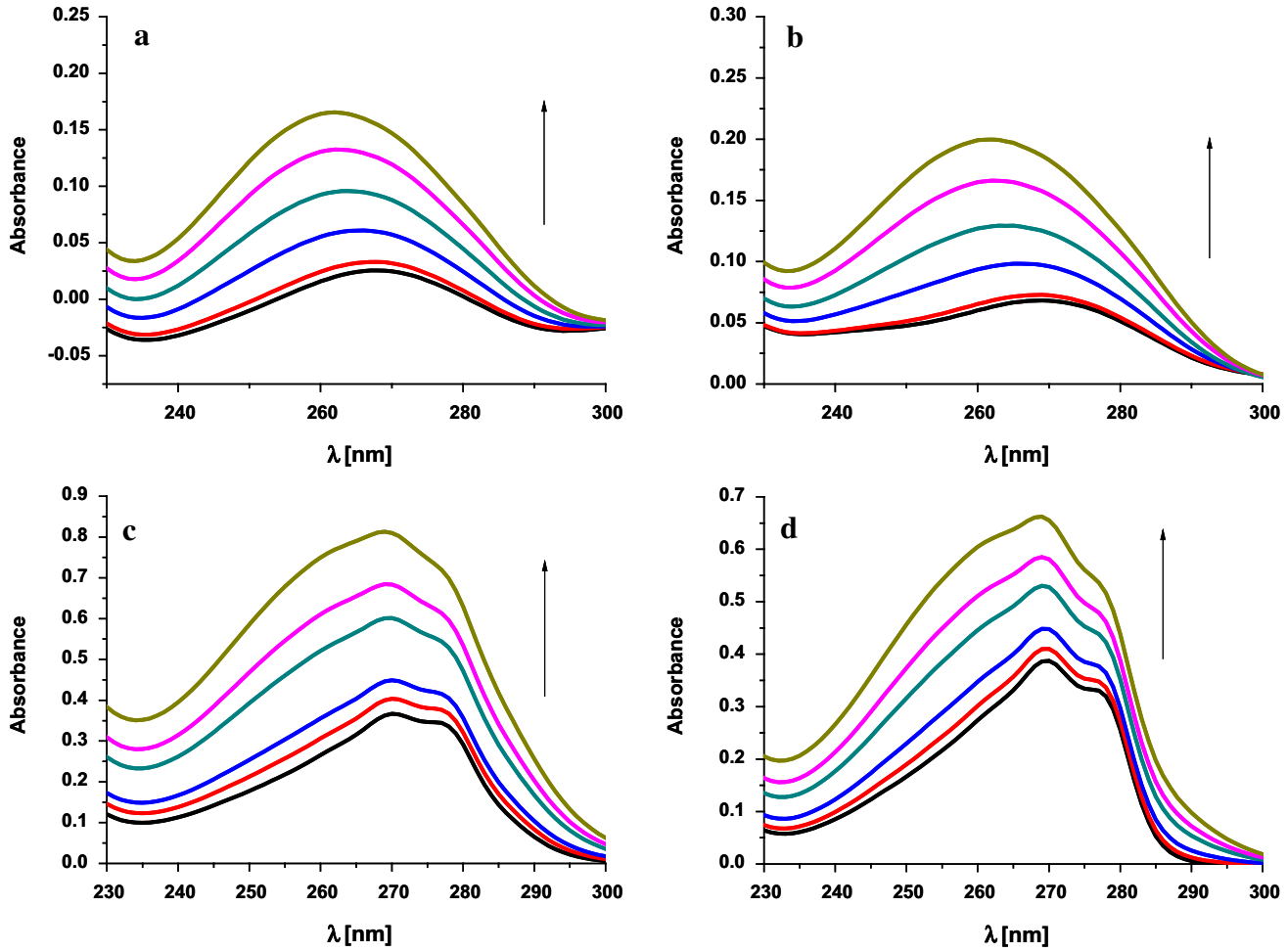

Fig. 7 Electronic absorption spectra of his^{6}dA ester (**a**), Cu(II)–his^{6}dA ester (**b**), his^{6}dA amide (**c**), Cu(II)–his^{6}dA amide (**d**) in the absence and in the presence of increasing amounts of DNA concentration. [Ligand] or [complex] = 10 μM, [DNA] = 0, 10, 50, 100, 150 and 200 μM. *Arrow* shows the absorbance changes upon increasing DNA concentration

Table 4 DNA binding constant (K_b), Stern–Volmer constant (K_{SV}), the apparent binding constant (K_{app}) and number of binding sites (n) for the ligands and their complexes with Cu(II)

Sample	K_{SV} (M^{-1})	K_b (M^{-1})	K_{app} (M^{-1})	N
his^{6}dA ester	1.58 (±0.06) × 10^2	8.11 (±0.06) × 10^3	Nd[a]	0.71 (±0.11)
Cu(II)–his^{6}dA ester	3.78 (±0.04) × 10^2	1.76 (±0.05) × 10^4	Nd[a]	0.99 (±0.09)
his^{6}dA amide	4.93 (±0.16) × 10^3	4.98 (±0.13) × 10^4	5.0 × 10^5	1.23 (±0.06)
Cu(II)–his^{6}dA amide	3,46 (±0.12) × 10^3	2.95 (±0.11) × 10^4	5.0 × 10^5	1.17 (±0.05)
his^{6}dA	4.12 (±0.03) × 10^1	Not determined	Nd[a]	0.51 (±0.06)
Cu(II)–his^{6}dA	3.06 (±0.05) × 10^2	Not determined	Nd[a]	0.54 (±0.08)

The standard deviations are in parenthesis

[a] 50 % decrease of fluorescence intensity was not observed

(**c**), Cu(II)–his^{6}dA amide (**d**), his^{6}dA (**e**) and Cu(II)–his^{6}dA (**f**) the fluorescence intensities of EB-DNA system show a decreasing trend with increasing concentration of studied samples, indicating that some EB molecules are released from EB-DNA after an exchange with the studied compounds which results in the fluorescence quenching of EB.

This may be due to that the studied compounds displace the EB from its DNA-binding sites in the competitive manner.

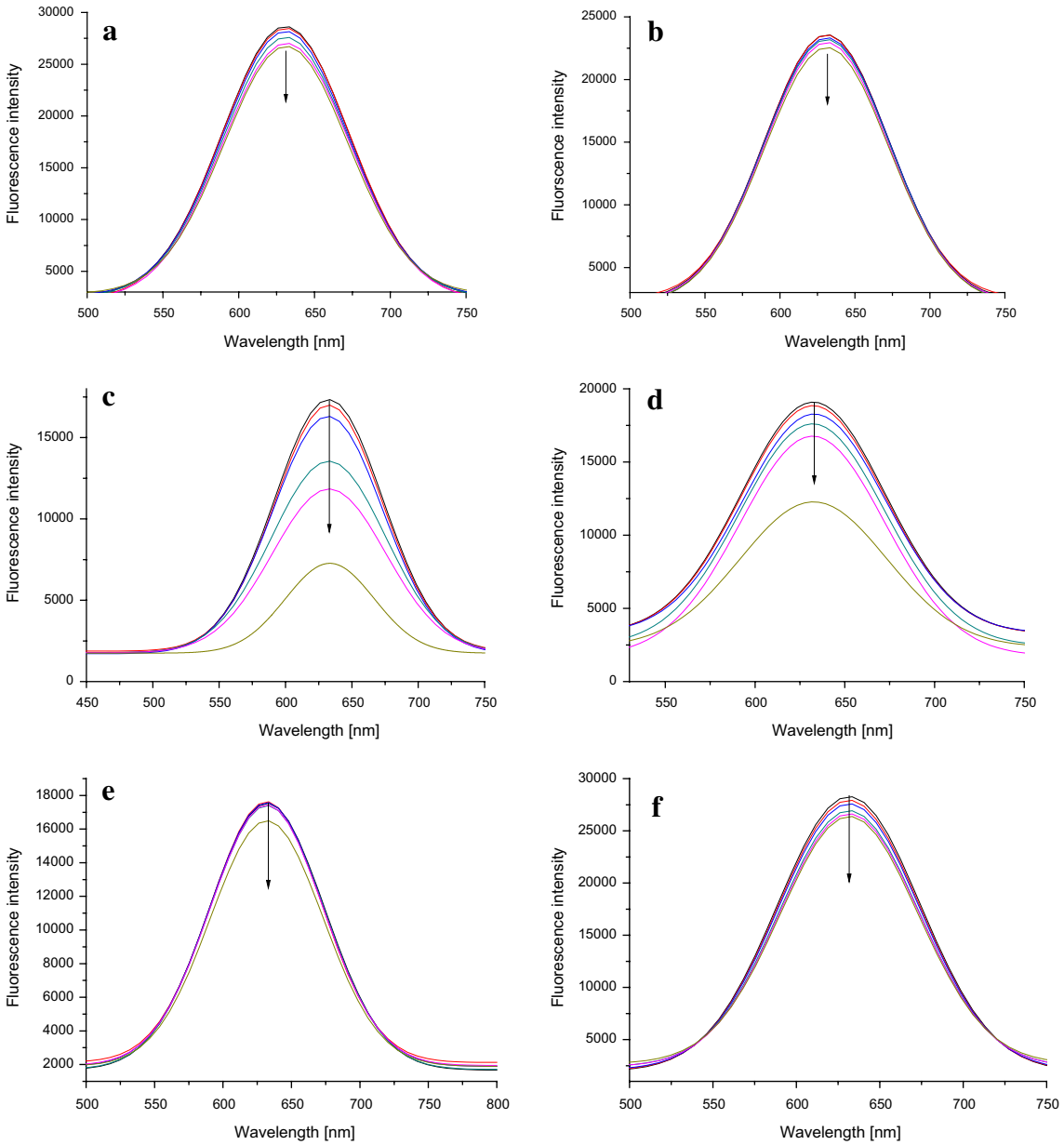

Fig. 8 Emission spectra of EB bound to DNA in absence and presence of ligands: his^{6}dA ester (**a**), his^{6}dA amide (**c**) and his^{6}dA (**e**) and complexes: Cu(II)–his^{6}dA ester (**b**), Cu(II)–his^{6}dA amide (**d**) and Cu(II)–his^{6}dA (**f**). [EB] = 10 μM, [DNA] = 25 μM, [ligand] or [complex] = 0, 10, 50, 100, 150, 200 μM. The *arrow* shows the intensity changes on increasing the ligand and complex concentration

In order to quantitatively compare this quenching behavior, the classical Stern–Volmer equation was employed. The plots (Fig. 9) illustrate that the quenching of EB bound to DNA are in good agreement with the linear Stern–Volmer equation.

The K_{SV} and the n values of his^{6}dA ester, his^{6}dA amide, his^{6}dA and complexes: Cu(II)–his^{6}dA ester, Cu(II)–his^{6}dA amide and Cu(II)–his^{6}dA (Table 4) indicate that these compounds show quenching efficiency and especially his^{6}dA amide and its copper complex have revealed significant degree of binding to DNA. The binding strength of his^{6}dA amide and Cu(II)–his^{6}dA amide (only those samples caused a 50 % decrease of fluorescence intensity) with DNA was characterized by using Eq. 3 to calculate the apparent binding constant (K_{app}). The K_{app} values of his^{6}dA amide and Cu(II)–his^{6}dA amide were estimated to be 5.0×10^5 M^{-1}, supporting a strong interaction of these compounds with DNA. It can be concluded that the binding of these compounds to CT-DNA may occur by partial intercalation, since their apparent binding constants are of the order characteristic for moderate intercalators [32, 33]. The results are consistent with those obtained from electronic absorption studies and point out significant influence of the groups $–NH_2$, $–OCH_3$ and –COOH

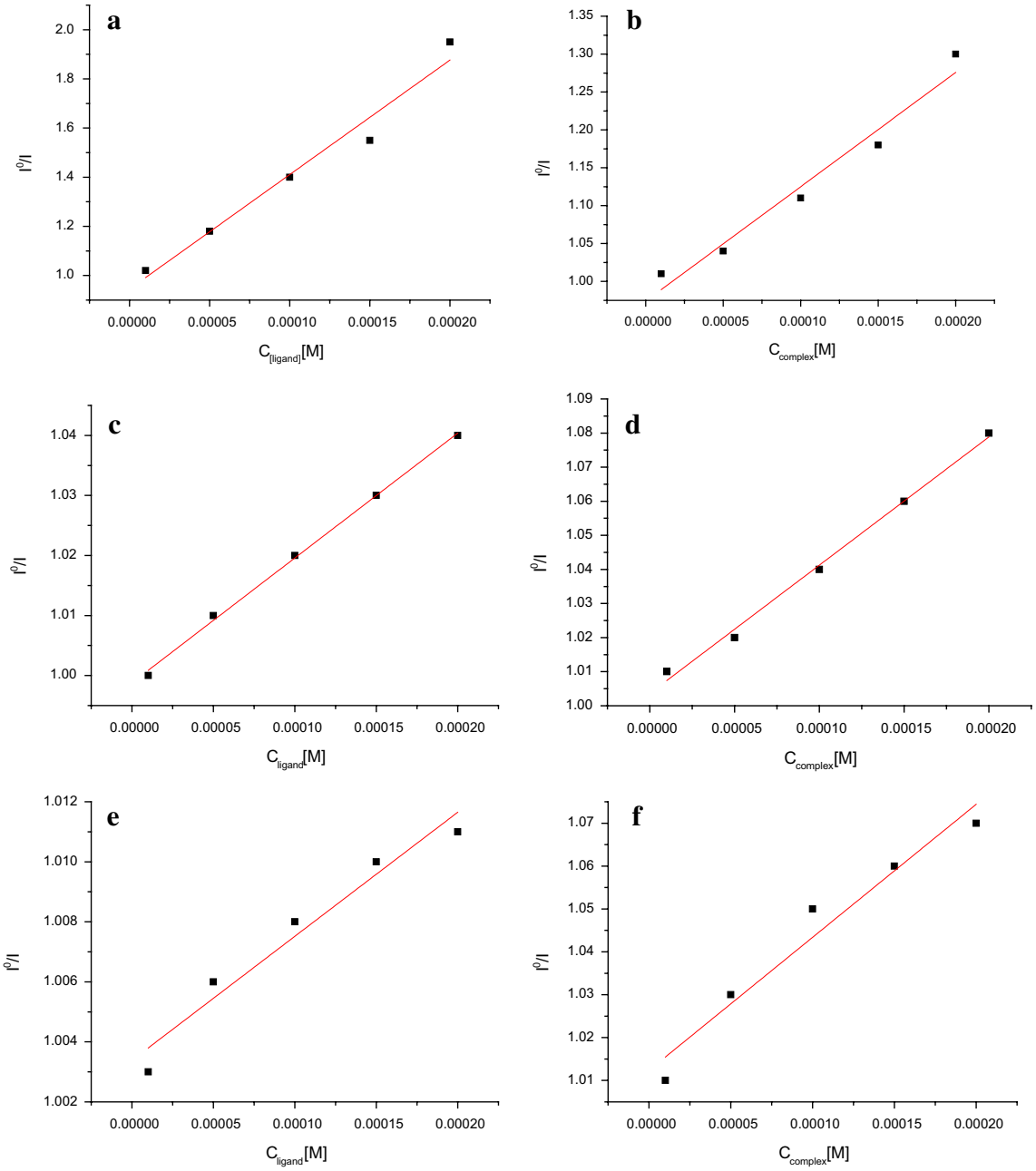

Fig. 9 Stern–Volmer plot of fluorescence titrations of the ligands: his^{6}dA ester (**a**), his^{6}dA amide (**c**) and his^{6}dA (**e**) and complexes: Cu(II)–his^{6}dA ester (**b**), Cu(II)–his^{6}dA amide (**d**) and Cu(II)–his^{6}dA (**f**)

on binding of the ligands/the complexes to DNA. Only the amide derivative and its complex reveal some intercalative ability. It may be supposed that they can acquire more helicoidal geometry which could facilitate intercalation.

Conclusion

2′-deoxyadenosines modified in purine part of the molecule with histidine moieties his^{6}dA ester and his^{6}dA amide exhibit the chelating ability towards copper(II) ions. The complexes of 1:2 (metal:ligand) stoichiometry are formed at a pH about 7. The $\{N(1), N_{am}^-, 2N_{im}\}$ coordination mode has been supported by spectroscopic parameters derived from electronic absorption, CD and EPR spectra. The binding ability of these complexes towards CT-DNA has been tested using different spectroscopic techniques. The results suggest that the ligands and the complexes can bind to CT-DNA via a groove-binding mode. The his^{6}dA amide and its complex have exhibited a greater binding propensity to

CT-DNA. The EB competition method has revealed that both of them are able to bind via intercalative manner as well. The K_{app} values calculated for these two systems are similar to those found for other intercalators which can be indicative of their tendency to act in this manner [28, 29]. The his^{6}dA ester, his^{6}dA and their Cu(II) complexes can only interact via groove-binding mode to the DNA double helix because the emission EB-DNA spectrum has been scarcely affected by adding these compounds to the solution. The difference of binding ability of the complexes can be derived from the differences of histidine residue incorporated in purine moiety of 2′-deoxyadenosine. All studied complexes promote cleavage of pEGFP-C1. Among the ligands only his^{6}dA has exhibited nuclease activity [6]. The possible cleavage mechanism can be hydrolytic pathway. Nucleosides modified with histidine moieties can provide "building blocks" of oligonucleotides in DNA sequence of deoxyribozymes which in the presence of copper ions may reveal potential for hydrolysis of complementary RNA.

Acknowledgments Financial support of this work by Statute Funds No. I28/DzS/9184.

References

1. Hadjiliadis N, Sletten E (eds) (2009) Metal complex-DNA interactions. Willey Publishing, Chippenham
2. Casassas E, Izguierdo-Ridorsa A, Tauler R (1990) J Inorg Biochem 39:327–336
3. Hollenstein M, Hipolito ChJ, Lam CH, Perrin DM (2009) ChemBioChem 10:1988–1992
4. Hollenstein M, Hipolito ChJ, Lam CH, Perrin DM (2009) Nucleic Acids Res 37:1638–1649
5. Smuga D, Majchrzak K, Sochacka E, Nawrot B (2010) New J Chem 34:934–948
6. Lodyga-Chruscinska E, Sierant M, Pawlak J, Sochacka E (2013) QScience 38:1–11
7. Irving HM, Miles MG, Pettit LD (1967) Anal Chim Acta 38:475–488
8. Gans P, Sabatini A, Vacca A (1985) J Chem Soc. Dalton Trans 6:1195
9. Alderighi L, Gans P, Ienco A, Peters D, Sabatini A, Vacca A (1999) Coord Chem Rev 184:311–318
10. Transformation protocol using heat shock MFT, 11/21/03. http://web.stanford.edu/~teruel1/Protocols/pdf/Transformation%20Protocol%20Using%20Heat%20Shock.pdf
11. Wolfe A, Shimer G, Meehan T (1987) Biochemistry 26:6392–6396
12. Jeyalkshmi K, Selvakumaran N, Bhuranesh NSP, Sreecanth A, Karvembu R (2014) RSC Adv 4:17179–17195
13. Ragheb MA, Eldesouki MA, Mohamed MS (2015) Spectrochim Acta Part A 138:585–595
14. Łodyga-Chruścińska E, Ołdziej S, Sochacka E, Korzycka K, Chruściński L, Micera G, Sanna D, Turek M, Pawlak J (2011) J Inorg Biochem 105:1212–1219
15. Sarathy RP, Ohrt JM, Chheda GB (1977) Biochemistry 16:4999–5008
16. Łodyga-Chruscinska E, Sochacka E, Smuga D, Chruściński L, Micera G, Sanna D, Turek M, Gąsiorkiewicz M (2010) J Inorg Biochem 104:570–575
17. Ren R, Yang P, Zheng W, Hua Z (2000) Inorg Chem 39:5454–5463
18. Kirin SI, Happel ChM, Hrubanova S, Weyhermüller T, Klein Ch, Metzler-Nolte N (2004) Dalton Trans 1201–1207. doi:10.1039/B313634E
19. Lodyga-Chruscinska E, Symonowicz M, Sykula A, Bujacz A, Garribba E, Rowinska-Zyrek M, Oldziej S, Klewicka E, Janicka M, Krolewska K, Cieslak M, Brodowska K, Chruscinski L (2015) J Inorg Biochem 143:34–47
20. González-Álvarez M, Alzuet G, Borrás J, Pitié M, Meunier B (2003) J Biol Inorg Chem 8:644–652
21. He J, Hu P, Wang Y-J, Tong M-L, Sun H, Mao ZW, Li L-N (2008) Dalton Trans 3207–3214. doi:10.1039/B801549J
22. Chen XQ, Peng XJ, Wang JY, Wang Y, Wu S, Zhang LZ, Wu T, Wu YK (2007) Eur J Inorg Chem 2007:5400–5407
23. Dimiza F, Perdih F, Tangoulis V, Turel I, Kessissoglou DP, Psomas G (2011) J Inorg Biochem 105:476–489
24. Mandal D, Chauhan M, Arjmand F, Aromi G, Ray D (2009) Dalton Trans 9183–9191. doi:10.1039/B909249H
25. Shahabadi N, Kashanian S, Khosravi M, Mahdavi M (2010) Transition Met Chem 35:699–705
26. Arjmand F, Jamsheera A, Mohapatra DK (2013) J Photochem Photobiol, B 121:75–85
27. Bei Q (2012) Chin J Struct Chem 31:1187–1193
28. Selvakumar B, Rajendiran V, Uma Maheswari P, Stoeckli-Evans H, Palaniandavar M (2006) J Inorg Biochem 100:316–330
29. Ramakrishnan S, Rajendiran V, Palaniandavar M, Periasamy VS, Srinag BS, Krishnamurthy H, Akbarsha MA (2009) Inorg Chem 48:1309–1322
30. Li XW, Li XJ, Li YT, Wu ZY, Yan CW (2013) J Photochem Photobiol B 118:22–32
31. Indumathy R, Radhika S, Kanthimathi M, Weyhermuller T, Nair BU (2007) J Inorg Biochem 101:434
32. Kahrovic E, Zahirovic A, Turkusic E (2014) J Chem Chem Eng 8:335–343
33. Qian J, Ma X, Tian J, Gu W, Shang J, Liu X, Yan S (2010) J Inorg Biochem 104:993–999